Supplement of Biogeosciences, 22, 7293–7308, 2025
https://doi.org/10.5194/bg-22-7293-2025-supplement

Biogeosciences Open Access EGU

Supplement of

Assessing the efficacy of river-based ocean alkalinity enhancement for carbon sequestration under high emission pathways

Xiao-Yuan Zhu et al.

Correspondence to: Wei-Lei Wang (weilei.wang@xmu.edu.cn)

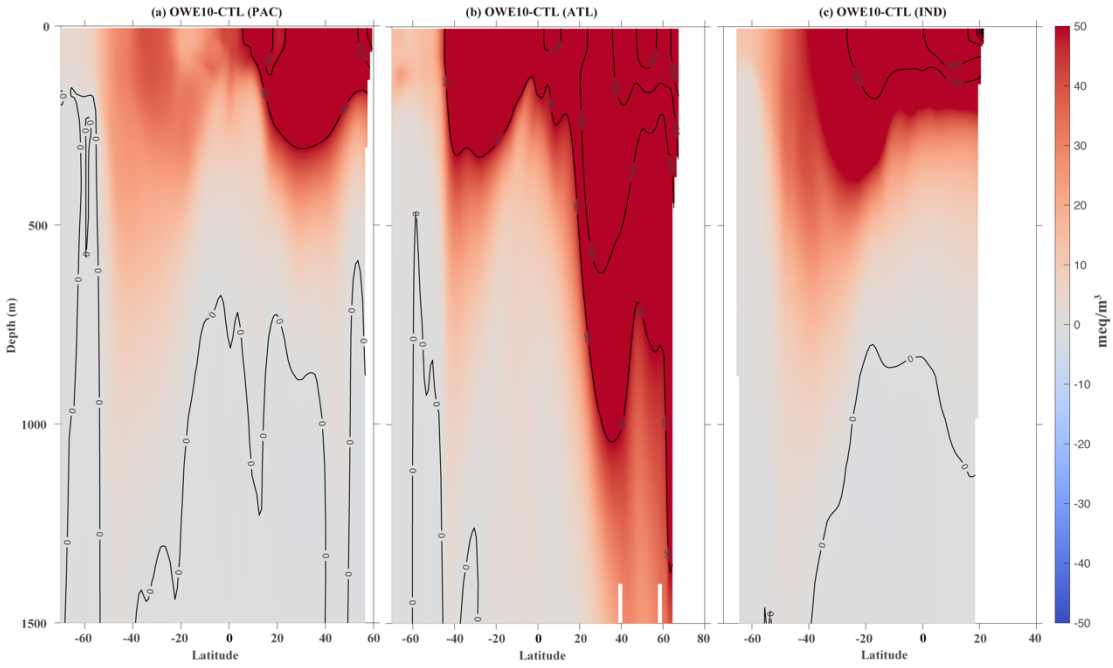

Figure S1. Vertical distribution of alkalinity anomaly along specific transects. (a) Differences between OWE10 and CTL along 150°W, representing the changes in the Pacific Ocean; (b) Differences between OWE10 and CTL along 30°W, representing the changes in the Atlantic Ocean; (c) Differences between OWE10 and CTL along 90°E, representing the changes in the Indian Ocean.

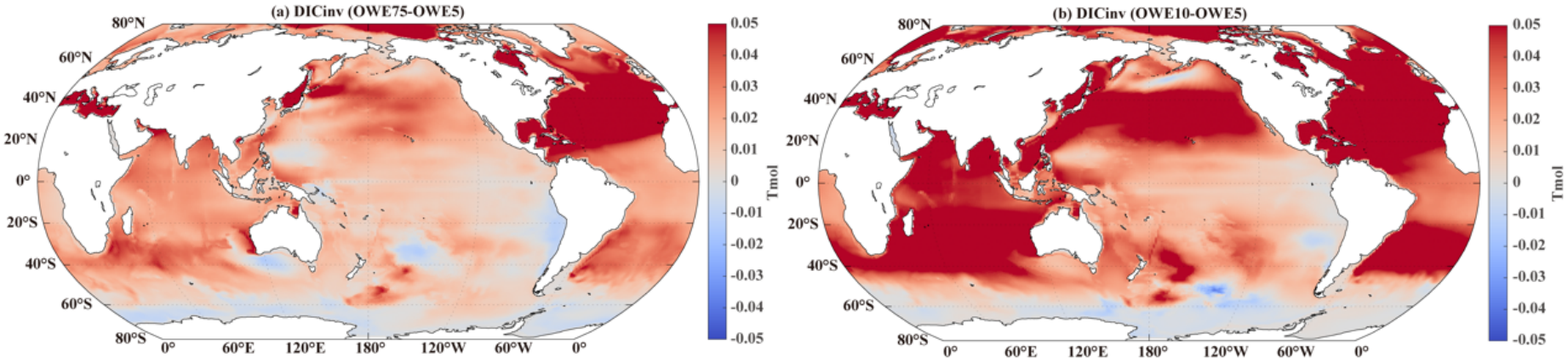

Figure S2. Anomaly of DIC inventory. (a) difference between OWE75 and OWE5; (b) difference between OWE10 and OWE5.

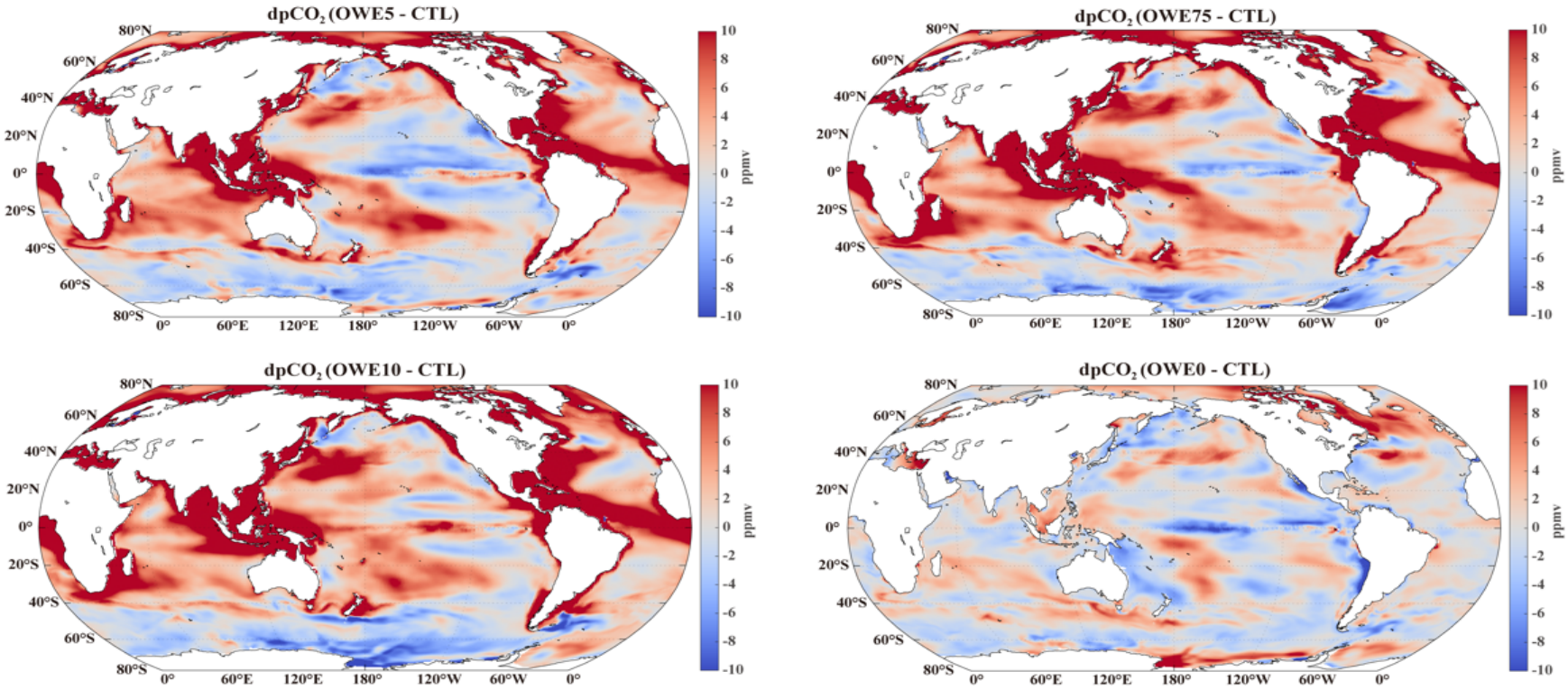

Figure S3. Anomaly of partial pressure of CO_2 between OAE simulations and the CTL in the last 10 years of the end of simulation. The partial pressure difference between the ocean and atmosphere is calculated by subtracting the pressure of CO_2 in the ocean from the pressure of CO_2 in the atmosphere.

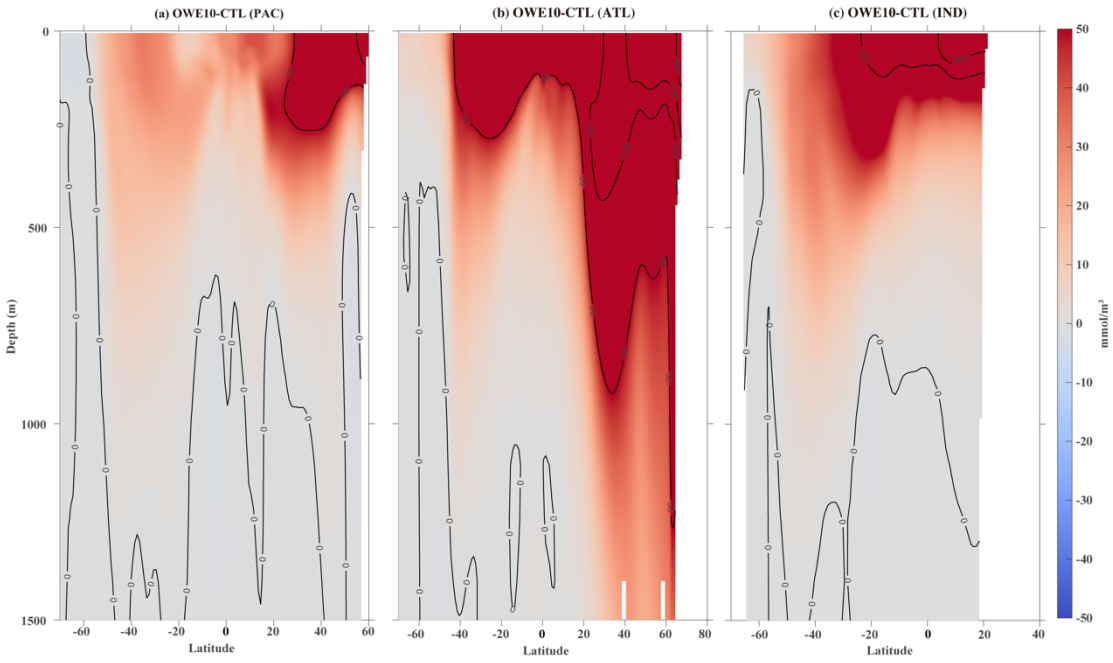

Figure S4. Vertical distribution of DIC concentration anomaly along 150°W (PAC), 30°W (ATL) and 90°E (IND) transects. (a) Differences between OWE10 and CTL along 150°W, representing the changes in the Pacific Ocean; (b) Differences between OWE10 and CTL along 30°W, representing the changes in the Atlantic Ocean; (c) Differences between OWE10 and CTL along 90°E, representing the changes in the Indian Ocean.

Video S1. Alkalinity anomaly under OWE0 compared to the CTL during simulation phase. Please refer to the ALK_bg2025_mp4.mp4 in the online Assets.

Video S2. Surface pH anomaly under OWE0 compared to the CTL during simulation phase. Please refer to the pH_bg2025_mp4.mp4 in the online Assets.